

LINC01012 upregulation promotes cervical cancer proliferation and migration via downregulation of CDKN2D

KEYI ZHANG*, XIAO NI*, XIAOLING MA*, RUI SUN, JIANGNAN QIU and CHENGYAN LUO

Department of Gynecology, The First Affiliated Hospital of Nanjing Medical University, Nanjing, Jiangsu 210036, P.R. China

Received August 21, 2022; Accepted January 12, 2023

DOI: 10.3892/ol.2023.13710

Abstract. The incidence and mortality of cervical cancer (CC) rank fourth among those of all gynecological malignancies. Long noncoding RNAs (lncRNAs) serve important roles in the development of various types of cancer. The aim of the present study was to explore the role of lncRNAs in the pathogenesis of CC and to identify novel therapeutic targets. LINC01012 was identified to be associated with an unfavorable prognosis in patients with CC based on bioinformatics analyses. Upregulated LINC01012 expression was further verified in CC samples and in cervical intraepithelial neoplasia grade 3 tissues compared with healthy tissues using reverse transcription-quantitative PCR. Functionally, following transfection with LINC01012 short hairpin RNA (sh-LINC01012), the proliferation and migration of CC cell lines were examined using 5-ethynyl-2'-deoxyuridine staining, colony formation and Transwell assays, which demonstrated that knockdown of LINC01012 in CC cells suppressed cell proliferation and migration *in vitro* and tumor growth in an *in vivo* xenograft model. The potential mechanisms of LINC01012 were further explored. A negative association between LINC01012 and cyclin dependent kinase inhibitor 2D (CDKN2D) was also identified based on The Cancer Genome Atlas data and this was confirmed using western blotting and rescue experiments. Consistently, knockdown of LINC01012 in CC cells upregulated CDKN2D expression. The inhibition of proliferation and migration of CC cells following transfection with sh-LINC01012 was reversed following co-transfection of sh-LINC01012 and CDKN2D short hairpin RNA. These findings suggested that upregulated LINC01012 expression in CC may stimulate the proliferation and migration of cancer

cells, thus promoting CC progression via downregulation of CDKN2D.

Introduction

As a prevalent gynecological tumor, cervical cancer (CC) endangers the health and lives of women due to its high mortality rates and poor prognoses (1). In 2020, there were 604,127 new cases of CC and 341,831 CC-associated deaths worldwide (2). Determining the pathogenesis is of importance in the timely diagnosis and management of CC. Previous evidence has shown that persistent high-risk human papillomavirus (hrHPV) infection can induce the carcinogenesis of CC (3). Furthermore, the interactions between oncogenes, and their association with hrHPV infections have been widely analyzed (4). Nevertheless, the exact molecular mechanisms involved in the progression and metastasis of CC remain largely unclear. Therefore, it is imperative to explore the pathogenesis and molecular mechanisms underlying the development of CC in order to identify effective diagnostic markers and therapeutic targets to improve its prognosis.

HPV encodes E6 and E7 proteins, which target TP53 and retinoblastoma proteins, respectively, and thus, disrupts cell-cycle progression, prevents apoptosis and enables the potentially transformed cells to replicate (5). Cell cycle progression from G₁ to S-phase is closely regulated by cyclin-dependent kinases (CDKs), such as CDK4/6 (6). CDK4/6 can be controlled via their subunits, including cyclin D and cyclin-dependent kinase inhibitors, which include the CDK interacting protein/kinase inhibitory protein and inhibitors of cyclin-dependent kinases (INK4) families (7). Cyclin dependent kinase inhibitor 2D (CDKN2D; also known as p19^{Ink4d}), a member of the INK4 family, functions as a key negative regulator of G₁/S transition (7). Aberrant CDKN2D expression has been demonstrated to contribute to the differentiation block and abnormal proliferation of malignant cells in multiple types of cancer, including pancreatic cancer, hepatocellular carcinoma and leukemia (8-10). However, to the best of our knowledge, it is unclear whether CDKN2D is involved in CC cell cycle progression and proliferation.

Long noncoding RNAs (lncRNAs) are non-coding RNAs >200 nucleotides in length. A previous study has demonstrated that lncRNAs are potentially involved in the development of malignant tumors (11). In particular, dysregulation of lncRNA expression can result in abnormally activated genes and

Correspondence to: Professor Chengyan Luo, Department of Gynecology, The First Affiliated Hospital of Nanjing Medical University, 368 North Jiangdong Road, Nanjing, Jiangsu 210036, P.R. China
E-mail: betteryuan66@163.com

*Contributed equally

Key words: LINC01012, cyclin dependent kinase inhibitor 2D, cervical cancer, proliferation, migration

pathways that trigger malignant tumor development (12,13). Additionally, lncRNAs are promising prognostic or diagnostic markers (14,15). The promoting effects of lncRNA SNHG1 and DLG1-AS1 on the malignant cellular behaviors of CC have been validated in previous studies (16,17).

The aim of the present study was to explore the roles of LINC01012 in CC. Public databases were analyzed using bioinformatic methods, and *in vitro* and *in vivo* experiments were performed to reveal the potential mechanism of LINC01012 in CC. The oncogenic role of LINC01012 might provide novel therapeutic targets for patients with CC.

Materials and methods

Data extraction and sample collection. The GSE75132 dataset (18), containing data for 20 female patients with persistent HPV16-infection and progression to cervical intraepithelial neoplasia grade 3 or CC (CIN3+), 10 female patients with persistent HPV16-infection without progression, and 11 HPV-negative female patients with normal cervix, was obtained from the Gene Expression Omnibus (GEO) database (<https://www.ncbi.nlm.nih.gov/geo/query/acc.cgi>). Differentially expressed genes between groups were screened by analyzing the GSE75132 dataset with packages 'limma' (version 3.54.0; <https://bioconductor.org/packages/release/bioc/html/limma.html>) (19) in R (version 4.0.4 for Windows 10; <https://mran.microsoft.com/snapshot/2021-03-21/bin/windows/base/>). In addition, data on LINC01012 expression and the clinical data of 304 patients with CC were obtained from The Cancer Genome Atlas (TCGA)-cervical squamous cell carcinoma and endocervical adenocarcinoma (CESC; <https://portal.gdc.cancer.gov/>). A total of 304 patients were stratified into low- or high-expression groups according to the auto-selected best cut-off value of LINC0102 mRNA level calculated using X-tile software (version 3.6.1; <https://x-tile.software.informer.com/>) (20). Afterwards, Kaplan-Meier (KM) analysis for overall survival was performed and the log-rank test was used to compare the prognosis between high- and low-expression of LINC0102 mRNA groups using R packages 'survival' (version 3.5.0; <https://CRAN.R-project.org/package=survival>) (21) and 'survminer' (version 0.4.8; <https://CRAN.R-project.org/package=survminer>) (22). Cervical cytology samples were obtained from 50 female patients with CC (median age, 57 years; age range, 39-65 years), 50 female patients with cervical intra-epithelial neoplasia grade 3 (CIN 3; (median age, 53 years; age range, 49-59 years) and 50 female patients with uterine myoma but normal cervix aged (median, 55 years; age range, 18-57 years) undergoing surgery at The First Affiliated Hospital of Nanjing Medical University (Nanjing, China) between January 2019 and January 2021. The cytology samples were used to examine LINC01012 expression by RT-qPCR. The inclusion criteria were: Histologically confirmed aforementioned diagnosis. Patients were excluded if they had other co-existing tumors or if they received previous chemotherapy or radiation.

The study was conducted in accordance with the Declaration of Helsinki (as revised in 2013) and approved by the Ethics Committee of First Affiliated Hospital of Nanjing Medical University (approval no. 2019-SR-373; Nanjing, China). All participants provided written informed consent.

The animal experiments were performed under a project license (approval no. F201844) granted by the Project of Maternal and Child Health of Jiangsu, in compliance with national and international guidelines, and approved by the Animal Care and Use Institutional Review Board of Nanjing Medical University (Nanjing, China). Additionally, the experiments were performed in accordance with the Animal Research: Reporting of *In Vivo* Experiments (ARRIVE) reporting checklist (23).

RNA extraction and reverse transcription-quantitative PCR (RT-qPCR). Total RNA was extracted from human CC cell lines (HeLa and SiHa) and cervical cytology samples using TRIzol® reagent (Invitrogen; Thermo Fisher Scientific, Inc.). Next, cDNA was synthesized by reverse transcription using a PrimeScript™ II 1st Strand cDNA synthesis kit (Takara Bio, Inc.) according to the manufacturer's protocol. RT-qPCR was then performed using SYBR Premix Ex Taq (Takara Bio, Inc.) according to the manufacturer's protocol. The thermocycling conditions were as follows: denaturation at 95°C for 10 min, followed by 45 cycles at 95°C for 30 sec and 68°C for 30 sec. U6 was used as the housekeeping gene. The relative mRNA level was determined using the comparative cycle threshold $2^{-\Delta\Delta C_q}$ method (24). The sequences of the primers were: LINC01012 forward, 5'-AAAAATCGGGAGGTGACGGG-3' and reverse, 5'-GCTTCCCGATGCACCTTTTC-3'; CDKN2D forward, 5'-AGTCCAGTCCATGACGCAG-3' and reverse, 5'-ATCAGGCACGTTGACATCAGC-3'; and U6 forward, 5'-CTCGCTTCGGCAGCAC-3' and reverse, 5'-AACGCTTCACGAATTTGCGT-3'.

Cell culture and transfection. Human CC cell lines (HeLa and SiHa) obtained from American Type Culture Collection were cultivated in DMEM (HyClone; Cytiva) containing 10% FBS (HyClone; Cytiva), 100 U/ml penicillin and 100 µg/ml streptomycin (HyClone; Cytiva) in a humidified cell culture chamber with 5% CO₂ at 37°C. The cells were passaged when cells reached 80% confluences and the medium was replaced every 2-3 days.

Lipofectamine® 2000 (Invitrogen; Thermo Fisher Scientific, Inc.) and pGPU6/GFP/Neo vector (Shanghai GenePharma Co. Ltd.) were used to transfect sh-LINC01012, sh-CDKN2D and non-targeting short hairpin RNA (sh-NC; all Shanghai GenePharma Co., Ltd.). The interval between infection and subsequent experimentation was 48 h. Briefly, cells were seeded in a 6-well plate at a density of 2x10⁵ cells per well, and the cell culture medium was replaced with antibiotic-free medium at 12 h prior to transfection. To transfect the cells, 2.5 µg transfection plasmid and 4 µl Lipofectamine® 2000 were separately dissolved in 200 µl OPTI-MEM for 5 min at room temperature, gently mixed, placed at room temperature for 20 min and added into the cell-containing medium. After 6 h of transfection at 37°C, the medium was replaced with fresh medium. Subsequently, the cells were cultivated for 48 h at 37°C and collected for *in vitro* experiments. The sequences of the transfection vectors were as follows: sh-LINC01012, 5'-GAACAATGT CAGATTGCAA-3'; sh-CDKN2D, 5'-GGTTATGTATCA GAAGAGA-3'; and sh-NC, 5'-UUCUCCGAACGUGUC ACGUTT-3'.

5-ethynyl-2'-deoxyuridine (EdU) assay and colony formation analysis. For the EdU assay, cells were seeded in a 96-well plate at a density of 3×10^3 cells per well and cultured overnight at 37°C. Subsequently, the cells were stained with 50 $\mu\text{mol/l}$ EdU solution (Guangzhou RiboBio Co., Ltd.) for 2 h at 37°C, fixed in 4% paraformaldehyde for 30 min and incubated with 2 mg/ml glycine for 5 min (both at room temperature). After washing once for 20 min in 0.5% Triton X-100 at room temperature, cells were labeled with 1X Apollo solution at room temperature for 30 min. Following washing three times for 10 min with PBS and 4% methanol at room temperature, nuclei were labeled with Hoechst 33342 solution at room temperature for 30 min in the dark. Images of EdU-stained cells (red), Hoechst33342-stained nuclei (blue) and merged images were captured under a fluorescence microscope at a magnification of x100 and analyzed using ImageJ software (ij153-win-java8; National Institutes of Health). The EDU-positive cell ratio was calculated using the following formula: Mean EDU positive cell numbers in each group/mean EDU positive cell numbers in sh-NC group.

For colony formation analysis, the HeLa and SiHa cells transfected with sh-LINC01012 or sh-NC for 48 h at 37°C were seeded in a 6-well plate at a density of 1×10^3 cells per well and cultivated for 14 days. When colonies reached a size of >50 cells, the cells were washed in PBS, fixed in 4% paraformaldehyde for 15 min at room temperature and dyed for 20 min in 0.1% crystal violet at room temperature. Images of colonies (definition, diameter of 0.3-1.0 mm) were captured under a light microscope for counting using ImageJ software (ij153-win-java8; National Institutes of Health). The relative number of colonies was calculated using the following formula: Mean colony number in each group/mean colony number in sh-NC group.

Transwell migration assay. Transwell inserts (pore size, 8 μm ; Corning, Inc.) without Matrigel-coating were used for the Transwell migration assay. The HeLa and SiHa cells (4×10^4 cells/well) transfected with sh-LINC01012, or sh-LINC01012 and sh-CDKN2D, or sh-NC were seeded in each insert with FBS-free DMEM. The inserts were placed in a 24-well plate with 500 μl DMEM supplemented with 10% FBS as an attractant in each lower chamber. After culture for 24 h at 37°C, the cells that migrated to the lower surface of the membrane were fixed in 4% paraformaldehyde for 15 min and dyed in 0.1% crystal violet solution (Beyotime Institute of Biotechnology) for 20 min (both at room temperature). After PBS washing and air drying, images of migratory cells were captured under a light microscope. The numbers of migrated cells in five random fields per sample were counted. The relative migrated cell ratio was calculated using the following formula: Mean migrated cell numbers in each group/mean migrated cell numbers in sh-NC group.

In vivo experiments. Eight female BALB/c nude mice (aged 5 weeks and weighed 16 g) were provided by Shanghai SLAC Laboratory Animal Co., Ltd. The animal experiments were approved by the Animal Care and Use Institutional Review Board of Nanjing Medical University (Nanjing, China) and carried out following the ARRIVE checklist. The mice were housed in a pathogen-free animal facility with a 12-h light-dark

cycle at a temperature of 20-24°C and a relative humidity of 50% and randomly assigned to the control group (sh-NC group) or sh-LINC01012 group (4 mice per group). The mice had free access to water and food. Animal health and behavior were monitored daily. Animal welfare was taken into consideration, including efforts to minimize suffering and distress, and use of analgesics according to the National Institutes of Health Guidelines for the Care and Use of Laboratory Animals (25). SiHa cells stably transfected with sh-NC or sh-LINC01012 were harvested and resuspended in PBS at 2×10^7 cells/ml. Cell suspension (100 μl ; 2×10^6 cells in total) was injected subcutaneously into the left axilla of the mice. Tumor size was measured every 3 days and tumor volumes were calculated using the following formula: $0.5 \times \text{length} \times \text{width}^2$. The mice were euthanized after anesthesia at 3 weeks after injection and the maximum diameter of tumor was measured. All mice were administered vaporized isoflurane (inhaled) for anesthesia at a concentration of 2.0% for induction and 1.0% for maintenance. Afterwards, the mice were sacrificed by rapid cervical dislocation. The mice with relaxed muscles were judged as dead when no breathing and no nerve reflex were observed. The xenograft tumors were harvested for further study including H&E and immunohistochemistry (IHC) staining.

H&E and IHC analysis. The xenograft tumors were fixed in 4% formaldehyde solution for 48 h at room temperature, then washed in distilled water for 45 sec, dehydrated with gradient ethanol (50, 70, 80, 95 and 100% respectively; 5 min each) at room temperature, embedded in paraffin at room temperature and cut into 4- μm -thick sections. The sections were deparaffinized in xylene for 5 min at room temperature, gradually hydrated using a descending alcohol series (100% for 3 min; 95, 70 and 50% for 3 min each) at room temperature and then washed in distilled water at room temperature. Afterwards, some of the sections for each sample were used for H&E staining, the others were for the IHC assay. For H&E staining, the slices were stained with hematoxylin for 5 min and with eosin for 3 min (both at room temperature). The pathological alterations of the tumors were observed under a light microscope.

For the IHC assay, the sections were incubated in 3% H_2O_2 solution in methanol at room temperature for 10 min to block endogenous peroxidase activity and washed with PBS for 5 min. Antigen retrieval was performed by incubation in 300 ml 10 mM citrate buffer with pH 6.0 and heating to 93°C for 10 min. The slides were cooled naturally at room temperature for 20 min and rinsed with PBS for 5 min. Antigen blocking was conducted by adding 100 μl FBS (10%) onto the slides and incubation at room temperature for 1 h. The slides were rinsed with PBS for 2 min. IHC analysis was carried out using KI-67 (1:800; sc-23900; Santa Cruz Biotechnology, Inc.) and E-cadherin (1:50; sc-8426; Santa Cruz Biotechnology, Inc.) primary antibodies to measure cellular proliferation and adhesion. Briefly, the sections were subsequently incubated with diluted primary antibodies overnight at 4°C and then washed with PBS. Afterwards, the slices were washed with PBS for 5 min and treated with peroxidase-conjugated secondary antibodies (1:1,000; PV-9000; OriGene Technologies, Inc.) for 2 h at 37°C and washed three times with PBS, 5 min each. After treatment with 3,3'-diaminobenzidine tetrahydrochloride

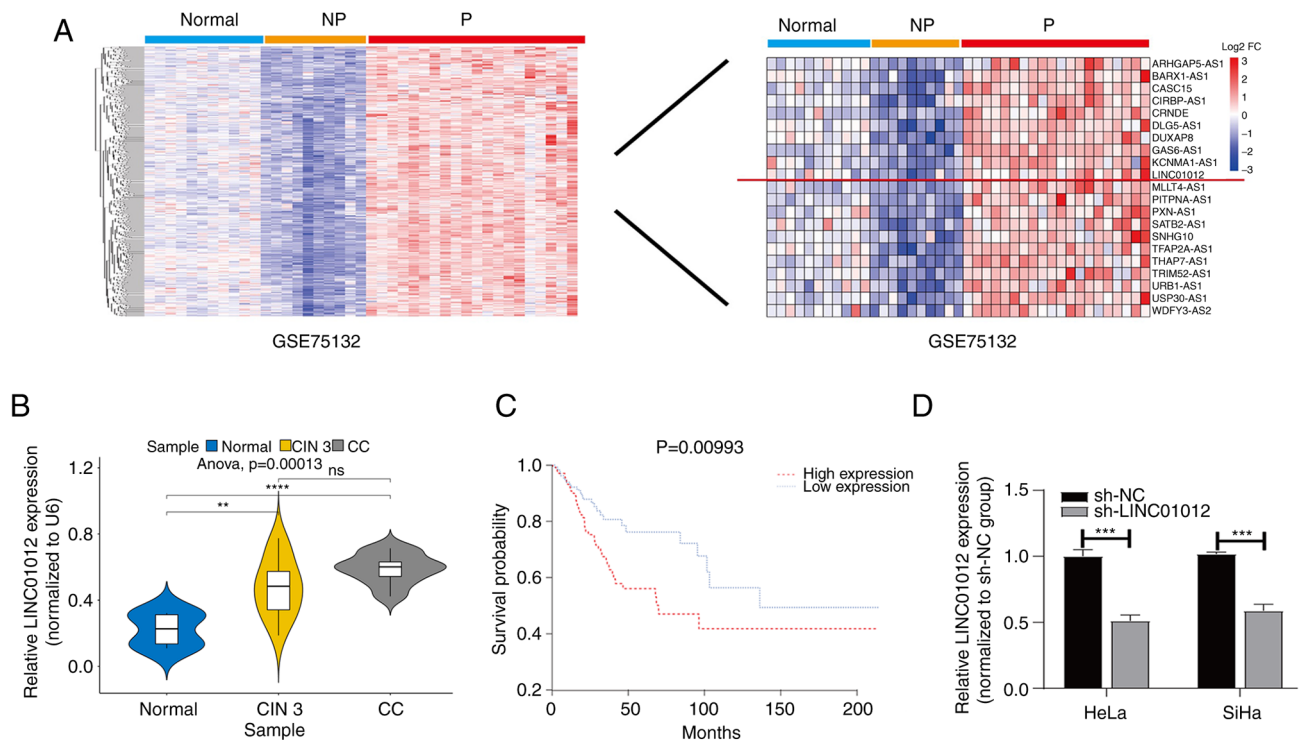


Figure 1. LINC01012 expression is upregulated in CC and its high expression is associated with an unfavorable prognosis. (A) Differentially expressed genes were identified using the 'limma' R package (based on \log_2 fold change >1 and a false discovery rate <0.05 threshold) in the GSE75132 dataset, and LINC01012 was identified to be upregulated in 20 samples from female patients with persistent HPV16-infection and progression to CIN 3+ compared with in samples from 10 female patients with persistent HPV16-infection without progression and 11 HPV-negative female patients with normal cervix (normal group). (B) Comparison of LINC01012 levels in cervical cytology samples from patients at The First Affiliated Hospital of Nanjing Medical University (Nanjing, China) with CC and CIN 3 with those with uterine myoma but normal cervix (normal group) ($n=50$ per group). Comparisons among multiple groups were performed by one-way ANOVA followed by Scheffe's post hoc test. **** $P<0.0001$, *** $P<0.001$ vs. normal group. (C) Kaplan-Meier survival analysis and log-rank test of LINC01012 expression in CC using data from The Cancer Genome Atlas. (D) LINC01012 levels in HeLa and SiHa cells transfected with sh-NC or sh-LINC01012. Differences between groups were analyzed using unpaired Student's t-test. **** $P<0.0001$ vs. sh-NC group. CC, cervical cancer; CIN 3+, cervical intraepithelial neoplasia grade 3 or cervical cancer; CIN 3, cervical intra-epithelial neoplasia grade 3; NP, persistent HPV16-infection without progression; ns, not significant; P, persistent HPV16-infection and progression to CIN 3+; \log_2 FC, \log_2 fold change; sh-NC, negative control short hairpin RNA; sh-LINC01012, LINC01012 short hairpin RNA.

(Sigma-Aldrich; Merck KGaA) solution at room temperature for 30 min, the sections were washed for 5 min and counter-stained with hematoxylin for 1 min at room temperature. Finally, the slides were dehydrated four times using alcohol (95, 95, 100 and 100%; 5 min each), soaked three times in xylene solution and sealed with a coverslip. Samples were observed and images were captured under a light microscope (magnification, $\times 100$; Olympus Corporation) and analyzed with ImageJ software (ij153-win-java8; National Institutes of Health).

Western blotting. Total protein was extracted from cells with RIPA lysis buffer (Beyotime Institute of Biotechnology) on ice. After measurement of the protein concentration using the BCA method, equal amounts of protein samples (20 μ g/lane) were separated by 10% SDS-PAGE and transferred onto polyvinylidene difluoride membranes (Millipore Sigma). The membranes were blocked in 5% skimmed milk for 1 h at room temperature, and immunoblotted with primary antibodies, including anti-CDKN2D (1:1,000; 10272-2-AP; Proteintech Group, Inc.) and anti-GAPDH (1:1,000; 10494-1-AP; Proteintech Group, Inc.) antibodies, at 4°C overnight, and HRP-conjugated secondary antibody (1:1,000, cat. no. sc271984; Santa Cruz Biotechnology, Inc.) at room

temperature for 1 h. Protein detection was achieved using an enhanced chemiluminescence detection kit (Millipore Sigma) and analyzed with ImageJ software (ij153-win-java8; National Institutes of Health).

Statistical analysis. The differentially expressed genes (\log_2 fold change >1 and false discovery rate <0.05) were identified using packages 'limma' (version 3.54.0; <https://bioconductor.org/packages/release/bioc/html/limma.html>) (19) in R (version 4.0.4 for Windows 10; <https://mran.microsoft.com/snapshot/2021-03-21/bin/windows/base/>). Pearson's correlation analysis was performed on LINC01012 and CDKN2D expression levels in TCGA-CESC dataset using R software. Kaplan-Meier (KM) survival analysis and the log-rank test were conducted with R packages to assess the prognostic potential of LINC01012 in CC using a RNA-Seq and clinical dataset (TCGA-CESC). The R packages 'survival' (version 3.5.0; <https://CRAN.R-project.org/package=survival>) (21) and 'survminer' (version 0.4.8; <https://CRAN.R-project.org/package=survminer>) (22) were employed for KM analysis.

All experiments were independently carried out at least three times, with samples in triplicate. SPSS 24.0 software (IBM Corp.) and GraphPad Prism 5.0 software (GraphPad Software; Dotmatics) were used for statistical analyses.

Data are presented as the mean \pm SD. Differences between groups were analyzed using unpaired Student's t-test or a Mann-Whitney U test. Comparisons among multiple groups were performed by one-way ANOVA followed by Scheffe's or Dunnett's post hoc test. $P < 0.05$ was considered to indicate a statistically significant difference.

Results

Upregulation of LINC01012 in CC and its prognostic significance. Through bioinformatics analysis of the GSE75132 dataset from the GEO database, differentially expressed LINC01012 was identified to be upregulated in persistent HPV16-infection and progression to CIN3+ samples compared with persistent HPV16-infection without progression and HPV-negative samples (Fig. 1A), and was also demonstrated to be upregulated in cervical cytology samples of CC and CIN 3 compared with the normal samples (Fig. 1B). A total of 304 patients with CC from TCGA were assigned into low- or high-expression groups according to the best cutoff value (-0.58) of LINC01012 mRNA level calculated using X-tile software. The association between LINC01012 expression and clinicopathologic characteristics is shown in Table SI, which showed that high LINC01012 expression in patients with CC was positively associated with advanced pathologic TNM stage. Furthermore, KM survival analysis using TCGA-CESC dataset revealed that high LINC01012 expression was associated with an unfavorable prognosis of CC ($P = 0.01$; log-rank test; Fig. 1C). Therefore, we hypothesized that LINC01012 might participate in the progression of CC and a series of experiments were designed to investigate this hypothesis.

LINC01012 knockdown suppresses proliferation and migration of CC cells *in vitro*. To explore the potential functions of LINC01012 in CC cells, LINC01012 was initially silenced by transfection of sh-LINC01012 in HeLa and SiHa cells and the transfection efficacy was validated by RT-qPCR (Fig. 1D). A series of functional experiments were then conducted to assess the biological functions of LINC01012 in CC cells. Transfection of sh-LINC01012 significantly reduced the EdU-positive cell ratio (Fig. 2A) and colony ratio both normalized to sh-NC group in CC cells (Fig. 2B), which indicated that LINC01012 knockdown suppressed cell proliferation and colony formation. In addition, the migration of CC cells was also inhibited following LINC01012 knockdown (Fig. 2C), as indicated by a Transwell migration assay.

LINC01012 regulates tumor growth of CC *in vivo*. A subcutaneous xenograft model was constructed to validate the biological function of LINC01012 *in vivo*. Consistent with the *in vitro* results, silencing LINC01012 by transfection with sh-LINC01012 significantly slowed down tumor growth as shown by comparing tumor volume at 3 weeks after injection in the sh-LINC01012 group with that in the sh-NC group (0.94 ± 0.17 vs. 0.41 ± 0.07 cm³, respectively; Fig. 3A). Fig. 3B shows the pathological features of the xenograft tumor examined using H&E staining under a light microscope. Furthermore, IHC assays confirmed that silencing LINC01012 decreased KI67 expression and

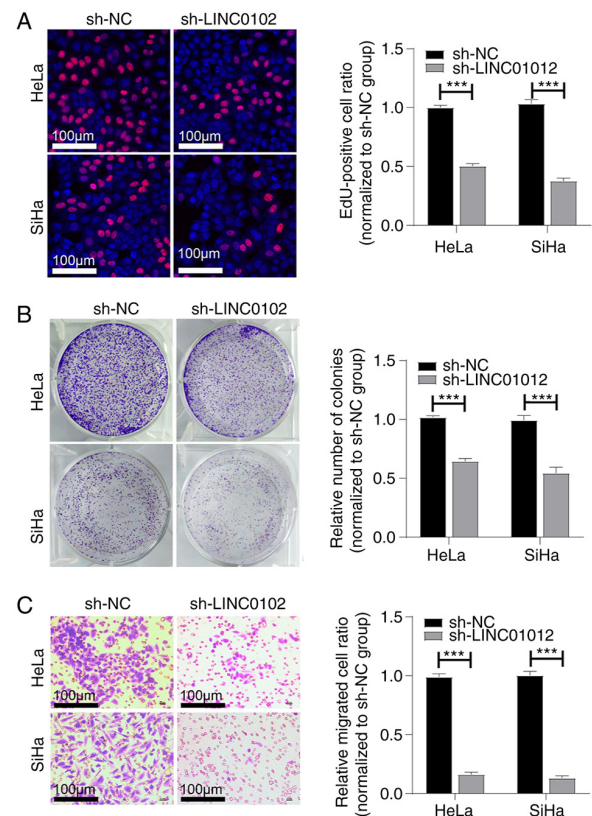


Figure 2. LINC01012 knockdown suppresses the proliferation and migration of cervical cancer cells *in vitro*. (A) LINC01012 knockdown reduced the EdU-positive cell ratio in HeLa and SiHa cells (magnification, $\times 100$). (B) LINC01012 knockdown reduced colony formation in HeLa and SiHa cells. (C) LINC01012 knockdown reduced the migration of HeLa and SiHa cells (Magnification, $\times 100$). *** $P < 0.001$ vs. sh-NC group. Differences between groups were analyzed using unpaired Student's t-test. EdU, 5-ethynyl-2'-deoxyuridine; sh-NC, negative control short hairpin RNA; sh-LINC01012, LINC01012 short hairpin RNA.

increased E-cadherin expression (Fig. 3C and D), indicating that LINC01012 knockdown inhibited the proliferation and promoted the adhesion of CC *in vivo*. Taken together, the aforementioned data demonstrated that LINC01012 could facilitate tumor growth by enhancing the proliferation and migration of CC cells, which further validated the oncogenic roles of LINC01012 in CC.

LINC01012 negatively regulates CDKN2D expression. By analyzing potential target genes regulated by LINC01012 in TCGA, CDKN2D was identified to be negatively weakly correlated with LINC01012 ($R = -0.19$; $P < 0.001$; Fig. 4A). Furthermore, the RNA and protein levels of CDKN2D were found to be upregulated in CC cells transfected with sh-LINC01012 (Fig. 4B and C), suggesting that LINC01012 could negatively regulate CDKN2D.

LINC01012 promotes proliferation and migration of CC cells by negatively regulating CDKN2D. sh-CDKN2D was used to further investigate whether CDKN2D serves a role in the effect of LINC0102 on CC development. The transfection efficiency is shown in Fig. S1. The protein levels of CDKN2D were also found to be downregulated in CC cells transfected with sh-CDKN2D (Fig. 5A). The protein expression levels

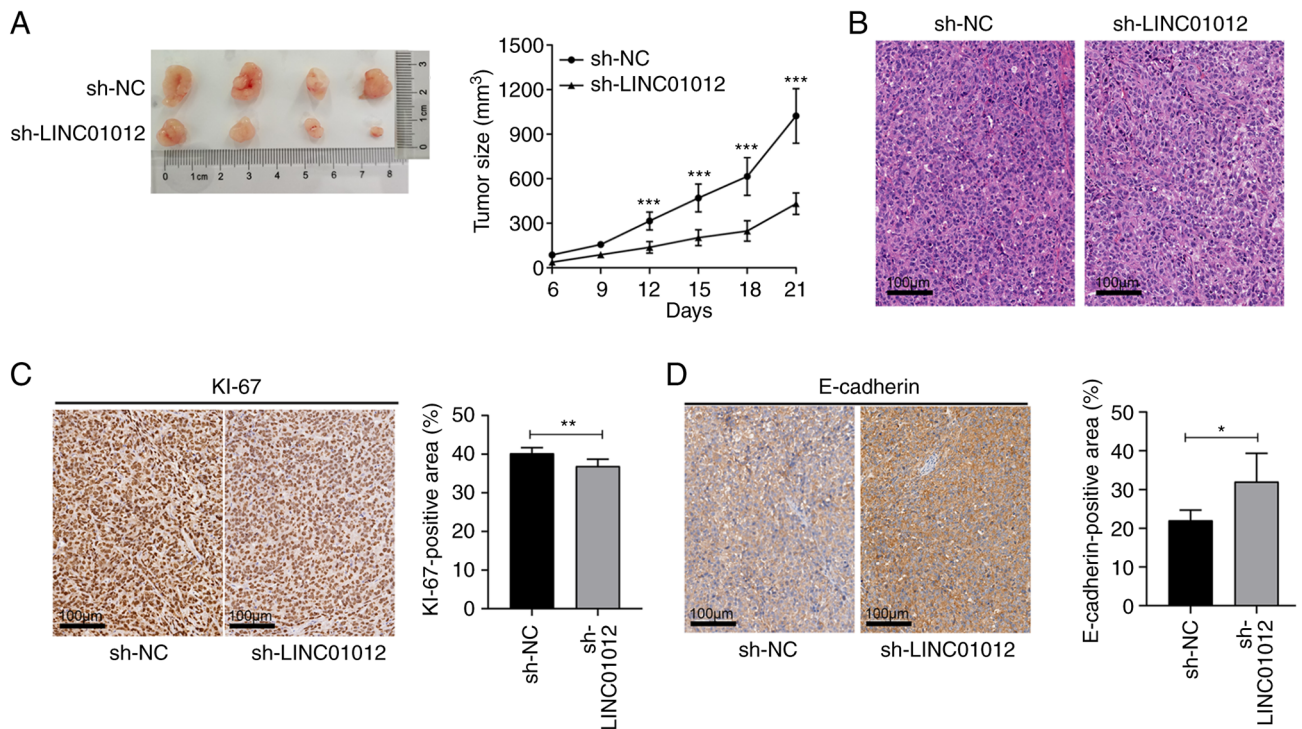


Figure 3. LINC01012 knockdown inhibits tumor growth by inhibiting proliferation and promoting adhesion of cervical cancer *in vivo*. (A) Tumor sizes were smaller in sh-LINC01012 group than in the sh-NC group. ***P<0.001 vs. tumor size in the sh-LINC01012 group at 12, 15, 18 and 21 days after injection of transfected SiHa cells. (B) H&E staining of the transplanted tumors (magnification, x100). Immunohistochemistry of (C) KI-67 and (D) E-cadherin of the transplanted tumors for the sh-LINC01012 and sh-NC groups (magnification, x100). Differences between groups were analyzed using unpaired Student's t-test. *P<0.05 vs. sh-NC group; **P<0.01 vs. sh-NC group. sh-NC, negative control short hairpin RNA; sh-LINC01012, LINC01012 short hairpin RNA.

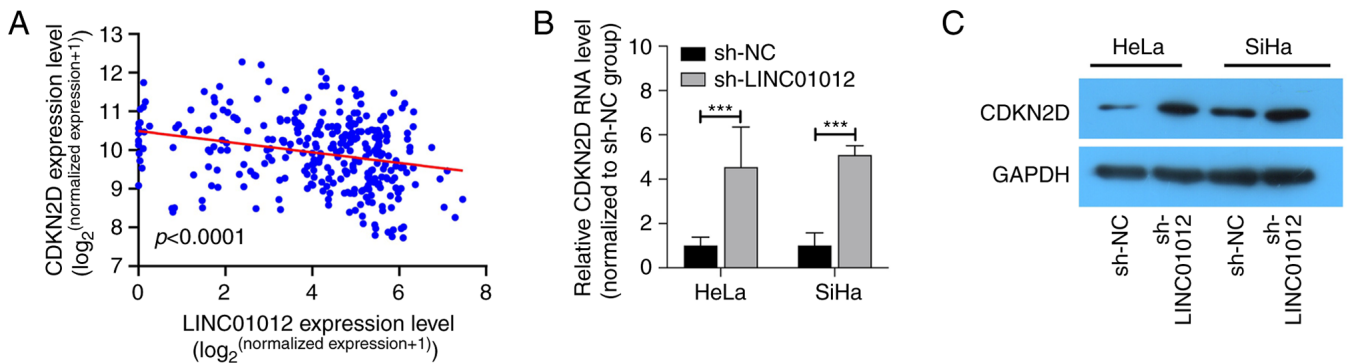


Figure 4. LINC01012 negatively regulates CDKN2D expression. (A) Weak negative correlation (R=-0.19; P<0.001) between the mRNA level of LINC01012 and that of CDKN2D as analyzed using The Cancer Genome Atlas. (B) LINC01012 knockdown upregulated CDKN2D RNA expression in HeLa and SiHa cells. (C) LINC01012 knockdown upregulated CDKN2D protein expression in HeLa and SiHa cells. Differences between groups were analyzed using unpaired Student's t-test. ***P<0.001 vs. sh-NC group. CDKN2D, cyclin dependent kinase inhibitor 2D; sh-NC, negative control short hairpin RNA; sh-LINC01012, LINC01012 short hairpin RNA.

of CDKN2D in HeLa and SiHa cells were upregulated after sh-LINC0102 transfection, which was partially reversed by co-transfection of sh-CDKN2D and sh-LINC0102 (Fig. 5C). The EdU-positive cell ratio was higher in CC cells with co-transfection of sh-LINC0102 and sh-CDKN2D compared with in those only with LINC0102 knockdown (Fig. 5B). The inhibited migration of CC cells following sh-LINC0102 transfection was consistently reversed by the knockdown of both LINC0102 and CDKN2D (Fig. 5D). These findings indicated that LINC0102 accelerated proliferation and migration of CC cells by downregulating CDKN2D.

Discussion

CC ranked fourth in terms of incidence and mortality among female malignancies worldwide in 2020 (2), and its pathogenesis remains incompletely understood. Although therapeutic strategies for CC, such as surgery, radiotherapy and chemotherapy, are continuously being improved, the 5-year survival rate of patients with advanced CC remains <50% worldwide in 2020 (2,26). Therefore, there is an urgent need to further explore the pathogenesis and identify novel target genes for the clinical treatment of CC.

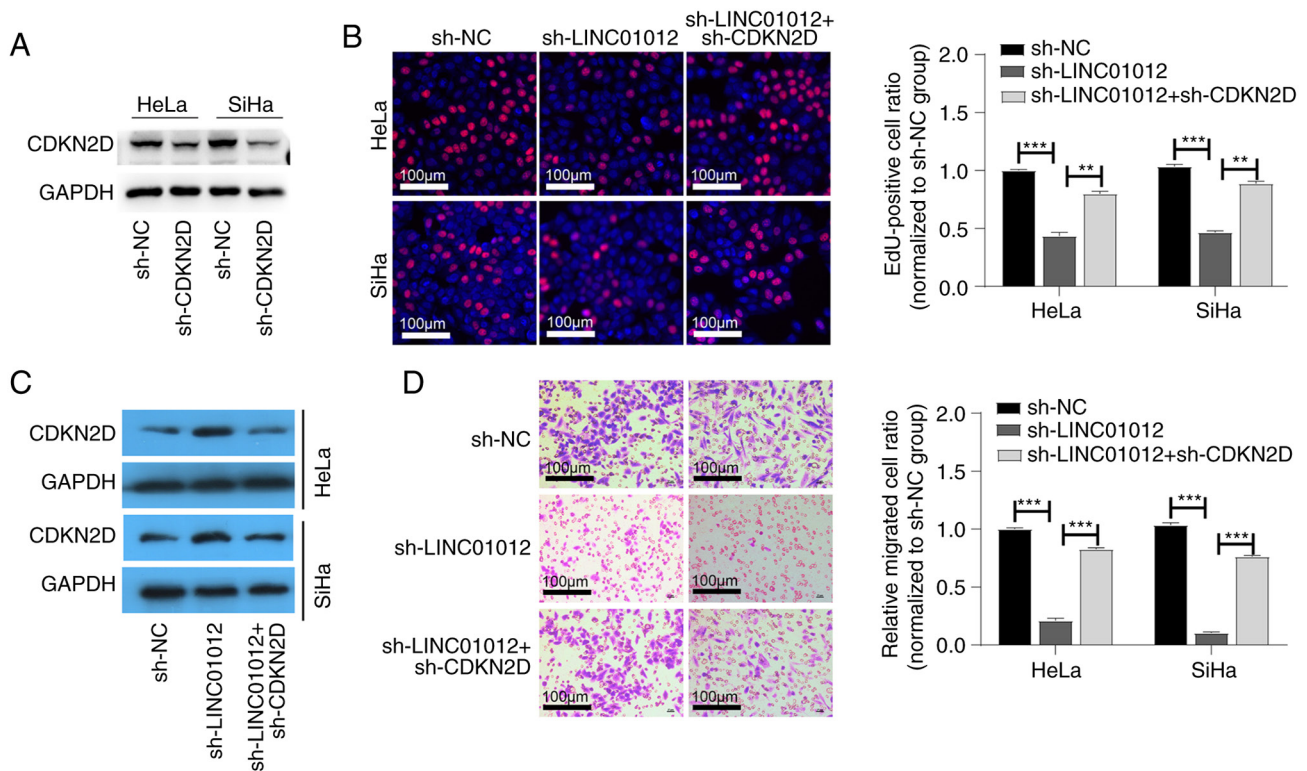


Figure 5. Inhibition of proliferation and migration of cervical cancer cells by transfection with sh-LINC01012 is reversed by CDKN2D knockdown. HeLa and SiHa cells were transfected with sh-NC, sh-LINC01012 or sh-LINC01012 + sh-CDKN2D. (A) CDKN2D protein expression in HeLa and SiHa cells after sh-CDKN2D transfection detected by western blotting. (B) EdU-positive cell ratio in HeLa and SiHa cells (magnification, x100). ** $P < 0.01$ vs. sh-LINC01012 group. *** $P < 0.001$ vs. sh-LINC01012 group. (C) CDKN2D protein expression in HeLa and SiHa cells after transfection with sh-LINC01012 or sh-LINC01012 + sh-CDKN2D detected by western blotting. (D) Migrated cell ratio in HeLa and SiHa cells (magnification, x100). Comparisons were performed by one-way ANOVA followed by Dunnett's post hoc test. ** $P < 0.01$ vs. sh-LINC01012 group. *** $P < 0.001$ vs. sh-LINC01012 group. CDKN2D, cyclin dependent kinase inhibitor 2D; sh-CDKN2D, CDKN2D short hairpin RNA; sh-NC, negative control short hairpin RNA; sh-LINC01012, LINC01012 short hairpin RNA.

lncRNAs are non-coding RNAs of >200 nucleotides that do not encode proteins (27). With the rapid progression in high-throughput sequencing techniques and bioinformatics analysis, a growing number of lncRNAs have emerged as functional regulators involved in various types of human cancer (28-30). lncRNAs participate in cancer development by promoting cell proliferation, migration and invasion (31), and have been revealed to exert pivotal roles by regulating target gene expression through cis- or trans-regulation (32).

To the best of our knowledge, the present study was the first to reveal that LINC01012 expression was upregulated in CC cytology samples. Survival analysis based on data obtained from TCGA revealed that high LINC01012 expression was associated with unfavorable prognosis of CC. *In vitro* experiments demonstrated that LINC01012 knockdown in CC cells significantly suppressed cell proliferation and migration. Consistent with the *in vitro* results, LINC01012 was found to promote tumor growth by increasing proliferation and migration of CC cells in a subcutaneous xenograft model.

Further analysis of TCGA data demonstrated that CDKN2D expression was negatively correlated with LINC01012 in CC specimens. Therefore, it was hypothesized that CDKN2D was involved in LINC01012-mediated oncogenesis. CDKN2D, located on chromosome 12p13, is a negative regulator of cell cycle progression (7). Its encoded protein is a member of the INK4 family and can form a stable complex with CDK4 or CDK6, thus preventing the activation

of CDKs and regulating G_1 phase progression (7). As a tumor-suppressor gene, CDKN2D is closely linked to tumor development by negatively regulating cell cycle progression (33-35). The *in vitro* assays performed in the present study demonstrated that the protein levels of CDKN2D were upregulated following LINC01012 knockdown in CC cells. Furthermore, the inhibited proliferation and migration of CC cells after LINC01012 knockdown were partially reversed by co-transfection with sh-LINC01012 and sh-CDKN2D. These findings indicated that LINC01012 accelerated the proliferation and migration of CC cells by downregulating CDKN2D expression. Taken together, the present findings demonstrated that LINC01012 could facilitate CC progression by targeting CDKN2D. The underlying mechanisms of LINC01012 regulating CDKN2D have not been investigated in the present study. Multiple signaling pathways have been revealed to be associated with tumorigenesis and progression of breast cancer, bladder cancer and CC. Among the pathways, the PI3K/Akt/mTOR signaling pathway has been demonstrated to be one of the most frequently activated signaling pathways (36). The specific signaling pathway downstream of LINC01012 and CDKN2D will be further explored in future studies. HeLa and SiHa cell lines were employed to explore the function and potential mechanism of LINC01012 *in vitro*. Nevertheless, other cells lines, including C33A, CaSki, HT-3 and human cervical epithelial cells, should be studied to further verify the conclusions.

In summary, to the best of our knowledge, the present study was the first to demonstrate that LINC01012 was upregulated in cervical cytology samples of CC and CIN 3 compared with in normal cervical tissues, and it was negatively associated with the overall survival of patients with CC. Upregulated LINC01012 expression in CC may stimulate the proliferation and migration of cancer cells both *in vitro* and *in vivo*, thus promoting the progression of CC by downregulating CDKN2D. The results of the present study indicated that LINC01012 may serve as a novel target for the management of CC.

Acknowledgements

The authors would like to thank Ms. Zhiwei Zhang (Department of Medical English, Nanjing Medical University, Nanjing, China) for their language editing assistance.

Funding

The present study was supported by Project of Maternal and Child Health of Jiangsu, P.R. China (grant no. F201844).

Availability of data and materials

The datasets used and/or analyzed during the current study are available from the corresponding author on reasonable request.

Authors' contributions

CL conceived and designed the study. KZ, XN and XM performed the experiments, collected the data, and drafted and reviewed the manuscript. RS and JQ contributed to the analysis and interpretation of the data. All authors reviewed the final manuscript and agreed to be accountable for all aspects of the work in ensuring that questions related to the accuracy or integrity of any part of the work are appropriately investigated and resolved. CL, KZ, XN and XM confirm the authenticity of all the raw data. All authors read and approved the final manuscript.

Ethics approval and consent to participate

The study was conducted in accordance with the Declaration of Helsinki (as revised in 2013). The study was approved by the Ethics Committee of First Affiliated Hospital of Nanjing Medical University (approval no. 2019-SR-373; Nanjing, China) and written informed consent was obtained from all individual participants. The animal experiments were performed under a project license (approval no. F201844) granted by the Project of Maternal and Child Health of Jiangsu, in compliance with national and international guidelines, and approved by the Animal Care and Use Institutional Review Board of Nanjing Medical University (Nanjing, China).

Patient consent for publication

Not applicable.

Competing interests

The authors declare that they have no competing interests.

References

1. Siegel RL, Miller KD and Jemal A: Cancer statistics, 2020. *CA Cancer J Clin* 70: 7-30, 2020.
2. Sung H, Ferlay J, Siegel RL, Laversanne M, Soerjomataram I, Jemal A and Bray F: Global cancer statistics 2020: GLOBOCAN estimates of incidence and mortality worldwide for 36 cancers in 185 countries. *CA Cancer J Clin* 71: 209-249, 2021.
3. Cohen PA, Jhingran A, Oaknin A and Denny L: Cervical cancer. *Lancet* 393: 169-182, 2019.
4. Crosbie EJ, Einstein MH, Franceschi S and Kitchener HC: Human papillomavirus and cervical cancer. *Lancet* 382: 889-899, 2013.
5. Hoppe-Seyler K, Bossler F, Braun JA, Herrmann AL and Hoppe-Seyler F: The HPV E6/E7 oncogenes: Key factors for viral carcinogenesis and therapeutic targets. *Trends Microbiol* 26: 158-168, 2018.
6. Bertoli C, Skotheim JM and de Bruin RA: Control of cell cycle transcription during G1 and S phases. *Nat Rev Mol Cell Biol* 14: 518-528, 2013.
7. Suryadinata R, Sadowski M and Sarcevic B: Control of cell cycle progression by phosphorylation of cyclin-dependent kinase (CDK) substrates. *Biosci Rep* 20: 243-255, 2010.
8. Zhu H, Gao Y, Wang Y, Liang C, Zhang Z and Chen Y: LncRNA CRNDE promotes the progression and angiogenesis of pancreatic cancer via miR-451a/CDKN2D axis. *Transl Oncol* 14: 101088, 2021.
9. Lee HA, Chu KB, Moon EK and Quan FS: Histone deacetylase inhibitor-induced CDKN2B and CDKN2D contribute to G2/M cell cycle arrest incurred by oxidative stress in hepatocellular carcinoma cells via forkhead box M1 suppression. *J Cancer* 12: 5086-5098, 2021.
10. Wang Y, Jin W, Jia X, Luo R, Tan Y, Zhu X, Yang X, Wang X and Wang K: Transcriptional repression of CDKN2D by PML/RAR α contributes to the altered proliferation and differentiation block of acute promyelocytic leukemia cells. *Cell Death Dis* 5: e1431, 2014.
11. Hosseini ES, Meryet-Figuiere M, Sabzalipoor H, Kashani HH, Nikzad H and Asemi Z: Dysregulated expression of long noncoding RNAs in gynecologic cancers. *Mol Cancer* 16: 107, 2017.
12. Hosono Y, Niknafs YS, Prensner JR, Iyer MK, Dhanasekaran SM, Mehra R, Pitchiaya S, Tien J, Escara-Wilke J, Poliakov A, *et al*: Oncogenic role of THOR, a conserved cancer/testis long non-coding RNA. *Cell* 171: 1559-1572.e20, 2017.
13. Mondal T, Juvvuna PK, Kirkeby A, Mitra S, Kosalai ST, Traxler L, Hertwig F, Wernig-Zorc S, Miranda C, Deland L, *et al*: Sense-antisense lncRNA pair encoded by locus 6p22.3 determines neuroblastoma susceptibility via the USP36-CHD7-SOX9 regulatory axis. *Cancer Cell* 33: 417-434.e7, 2018.
14. Li C, Wang S, Xing Z, Lin A, Liang K, Song J, Hu Q, Yao J, Chen Z, Park PK, *et al*: A ROR1-HER3-lncRNA signalling axis modulates the Hippo-YAP pathway to regulate bone metastasis. *Nat Cell Biol* 19: 106-119, 2017.
15. Lin A, Hu Q, Li C, Xing Z, Ma G, Wang C, Li J, Ye Y, Yao J, Liang K, *et al*: The LINK-A lncRNA interacts with PtdIns(3,4,5)P₃ to hyperactivate AKT and confer resistance to AKT inhibitors. *Nat Cell Biol* 19: 238-251, 2017.
16. Liu Y, Yang Y, Li L, Liu Y, Geng P, Li G and Song H: LncRNA SNHG1 enhances cell proliferation, migration, and invasion in cervical cancer. *Biochem Cell Biol* 96: 38-43, 2018.
17. Rui X, Xu Y, Huang Y, Ji L and Jiang X: LncRNA DLG1-AS1 promotes cell proliferation by competitively binding with miR-107 and up-regulating ZHX1 expression in cervical cancer. *Cell Physiol Biochem* 49: 1792-1803, 2018.
18. Manawapat-Klopfer A, Thomsen LT, Martus P, Munk C, Russ R, Gmuender H, Frederiksen K, Haedicke-Jarboui J, Stubenrauch F, Kjaer SK and Iftner T: TMEM45A, SERPINB5 and p16INK4A transcript levels are predictive for development of high-grade cervical lesions. *Am J Cancer Res* 6: 1524-1536, 2016.
19. Ritchie ME, Phipson B, Wu D, Hu Y, Law CW, Shi W and Smyth GK: limma powers differential expression analyses for RNA-sequencing and microarray studies. *Nucleic Acids Res* 43: e47, 2015.
20. Camp RL, Dolled-Filhart M and Rimm DL: X-tile: A new bio-informatics tool for biomarker assessment and outcome-based cut-point optimization. *Clin Cancer Res* 10: 7252-7259, 2004.
21. Terry MT and Patricia MG: Modeling survival data: Extending the cox model. Springer, New York, ISBN 0-387-98784-3, pp261-287, 2000.
22. Kassambara A, Kosinski M and Biecek P: Drawing survival curves using 'ggplot2' [r package survminer version 0.4.8], 2020.

23. Percie du Sert N, Hurst V, Ahluwalia A, Alam S, Avey MT, Baker M, Browne WJ, Clark A, Cuthill IC, Dirnagl U, *et al*: The ARRIVE guidelines 2.0: Updated guidelines for reporting animal research. *PLoS Biol* 18: e3000410, 2020.
24. Livak KJ and Schmittgen TD: Analysis of relative gene expression data using real-time quantitative PCR and the 2(-Delta Delta C(T)) method. *Methods* 25: 402-408, 2001.
25. National Research Council (US) Committee for the Update of the Guide for the Care and Use of Laboratory Animals: Guide for the Care and Use of Laboratory Animals. 8th edition. National Academies Press, Washington, DC, 2011.
26. Lontos M, Kyriazoglou A, Dimitriadis I, Dimopoulos MA and Bamias A: Systemic therapy in cervical cancer: 30 Years in review. *Crit Rev Oncol Hematol* 137: 9-17, 2019.
27. Mercer TR, Dinger ME and Mattick JS: Long non-coding RNAs: Insights into functions. *Nat Rev Genet* 10: 155-159, 2009.
28. Liu W, Wang Z, Liu L, Yang Z, Liu S, Ma Z, Liu Y, Ma Y, Zhang L, Zhang X, *et al*: LncRNA Malat1 inhibition of TDP43 cleavage suppresses IRF3-initiated antiviral innate immunity. *Proc Natl Acad Sci USA* 117: 23695-23706, 2020.
29. Ma Y, Yang Y, Wang F, Moyer MP, Wei Q, Zhang P, Yang Z, Liu W, Zhang H, Chen N, *et al*: Long non-coding RNA CCAL regulates colorectal cancer progression by activating Wnt/ β -catenin signalling pathway via suppression of activator protein 2 α . *Gut* 65: 1494-1504, 2016.
30. Zhang ZW, Chen JJ, Xia SH, Zhao H, Yang JB, Zhang H, He B, Jiao J, Zhan BT and Sun CC: Long intergenic non-protein coding RNA 319 aggravates lung adenocarcinoma carcinogenesis by modulating miR-450b-5p/EZH2. *Gene* 650: 60-67, 2018.
31. Chi Y, Wang D, Wang J, Yu W and Yang J: Long non-coding RNA in the pathogenesis of cancers. *Cells* 8: 1015, 2019.
32. Hu G, Niu F, Humburg BA, Liao K, Bendi S, Callen S, Fox HS and Buch S: Molecular mechanisms of long noncoding RNAs and their role in disease pathogenesis. *Oncotarget* 9: 18648-18663, 2018.
33. Felisiak-Golabek A, Dansonka-Mieszkowska A, Rzepecka IK, Szafron L, Kwiatkowska E, Konopka B, Podgorska A, Rembiszewska A and Kupryjanczyk J: p19(INK4d) mRNA and protein expression as new prognostic factors in ovarian cancer patients. *Cancer Biol Ther* 14: 973-981, 2013.
34. Zang WQ, Yang X, Wang T, Wang YY, Du YW, Chen XN, Li M and Zhao GQ: MiR-451 inhibits proliferation of esophageal carcinoma cell line EC9706 by targeting CDKN2D and MAP3K1. *World J Gastroenterol* 21: 5867-5876, 2015.
35. Bartkova J, Thullberg M, Rajpert-De Meyts E, Skakkebaek NE and Bartek J: Lack of p19INK4d in human testicular germ-cell tumours contrasts with high expression during normal spermatogenesis. *Oncogene* 19: 4146-4150, 2000.
36. Alzahrani AS: PI3K/Akt/mTOR inhibitors in cancer: At the bench and bedside. *Semin Cancer Biol* 59: 125-132, 2019.



This work is licensed under a Creative Commons Attribution-NonCommercial-NoDerivatives 4.0 International (CC BY-NC-ND 4.0) License.